

**Titre:** Spectral effects and enhancement quantification in healthy human saliva with surface-enhanced Raman spectroscopy using silver nanopillar substrates. Supplément  
**Title:**

**Auteurs:** Esmat Zamani, Nassim Ksantini, Guillaume Sheehy, Katherine J. I. Ember, Bill Baloukas, Oleg Zabeida, Trang Tran, Myriam Mahfoud, Jolanta-Ewa Sapieha, Ludvik Martinu, & Frédéric Leblond  
**Authors:**

**Date:** 2024

**Type:** Article de revue / Article

**Référence:** Zamani, E., Ksantini, N., Sheehy, G., Ember, K. J. I., Baloukas, B., Zabeida, O., Tran, T., Mahfoud, M., Sapieha, J.-E., Martinu, L., & Leblond, F. (2024). Spectral effects and enhancement quantification in healthy human saliva with surface-enhanced Raman spectroscopy using silver nanopillar substrates. *Lasers in Surgery and Medicine*, 56(2), 206-217. <https://doi.org/10.1002/lsm.23746>  
**Citation:**

 **Document en libre accès dans PolyPublie**  
Open Access document in PolyPublie

**URL de PolyPublie:** <https://publications.polymtl.ca/57325/>  
**PolyPublie URL:**

**Version:** Matériel supplémentaire / Supplementary material  
Révisé par les pairs / Refereed

**Conditions d'utilisation:** Creative Commons Attribution-Utilisation non commerciale 4.0  
**Terms of Use:** International / Creative Commons Attribution-NonCommercial 4.0  
International (CC BY-NC)

 **Document publié chez l'éditeur officiel**  
Document issued by the official publisher

**Titre de la revue:** Lasers in Surgery and Medicine (vol. 56, no. 2)  
**Journal Title:**

**Maison d'édition:** Wiley  
**Publisher:**

**URL officiel:** <https://doi.org/10.1002/lsm.23746>  
**Official URL:**

**Mention légale:**  
**Legal notice:**

1 **Appendix A: Supplemental Material**

2 The substrates were prepared on Si <100> wafers and glass slides using a two-step process: 1)  
3 by first growing a thin 50-nm-thick Ag mirror at normal incidence ( $0^\circ$ ) of arriving Ag atoms,  
4 2) by tilting the Ag mirrors at an incidence angle of  $85^\circ$  during the deposition. The first step is  
5 illustrated in Fig. 6 and the second step is illustrated in Fig 7.



6

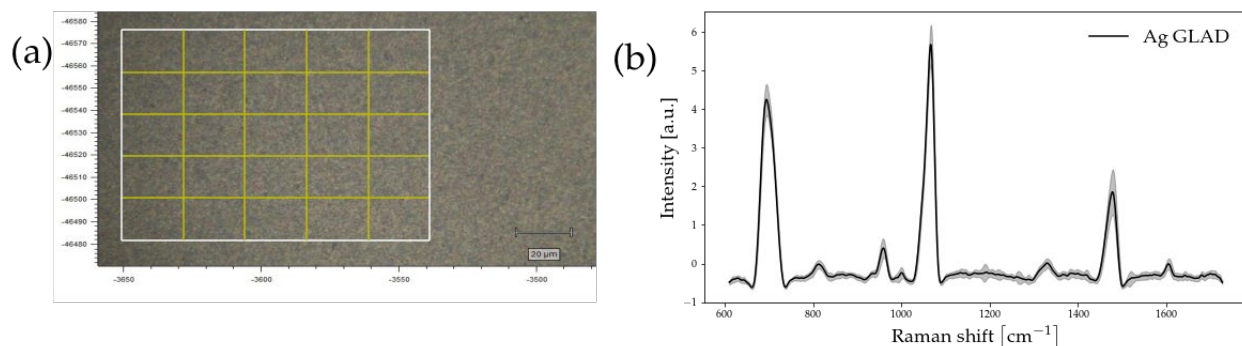
7 **Fig. 6** Ag Mirror finished substrate before the GLAD deposition.



8

9 **Fig. 7** Ag mirror substrates in the deposition chamber, inclined such that the deposition will result in a GLAD finished  
10 substrate.

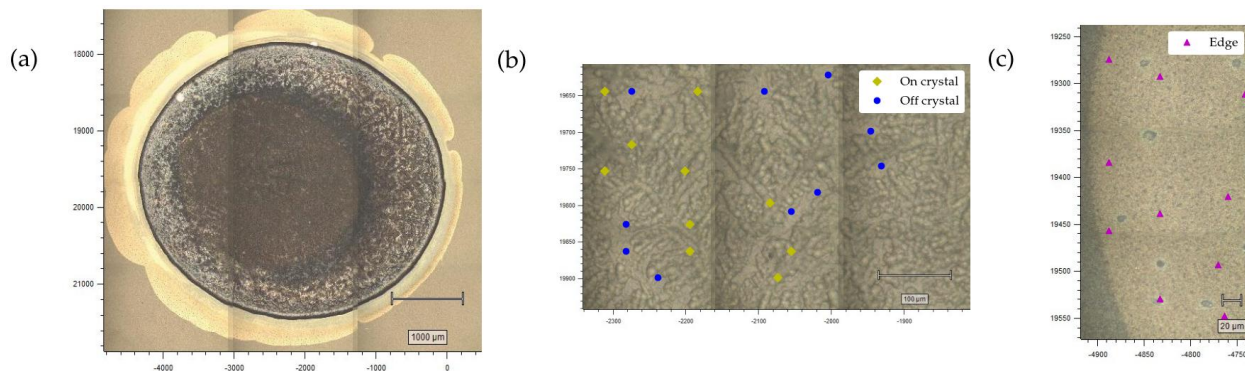
11 Figure 8 illustrates the average spatial Raman signal of an Ag GLAD substrate, over a 6x6 map  
12 grid, spanning an approximate 100µm x 100 µm area.



13

14 **Fig. 8** Average substrate spatial variability. (a) 50x brightfield snapshot of an Ag GLAD substrate with a 6x6 map grid,  
15 spanning an approximate 100µm x 100 µm area. (b) Average SNV Raman signal with the standard deviation of the  
16 6x6 rectangular map.

17 Figure 9 illustrates the SERS workflow with a commercial Raman microscope, starting with a  
18 5x brightfield snapshot, followed with a 50x snapshot of the *Center* region and the *Edge* region,  
19 and the acquisition of a point map distribution in for the given morphological regions (*Edge*,  
20 *On crystal* and *Off crystal*).



21 **Fig. 9** SERS workflow with a commercial Raman microscope. (a) 5x brightfield snapshot of a 10 µL dried saliva  
22 droplet on an Ag GLAD substrate. (b) 50x brightfield snapshot of the *Center* region of the same droplet with a 10  
23 points map distribution. (c) 50x brightfield snapshot of the *Edge* region of the same droplet with a 10 points map  
24 distribution.

25 The tentative band assignment of the Raman bands of human saliva reported in Table 2 is based  
26 on the spectral bands of the model saliva [6,79] and previous studies available in the literature  
27 [6,76–78].

Table 2. Tentative band assignment of saliva based on an artificial model saliva.

Raman peak [cm <sup>-1</sup> ]	SERS peak [cm <sup>-1</sup> ]	Location of peak in model saliva	Location of peak in human saliva supernatant	Band assignment based in peak position from constituents of model saliva	Additional possible contributions to bands from literature
623	625	<i>Edge</i>	<i>Edge, Center</i>	Protein (phenylalanine) or uric acid	-
646	647	<i>Edge</i>	<i>Edge, Center</i>	Protein (tyrosine, phenylalanine), glucose	-
731	729	Undetected	<i>Edge, Center</i>	-	Adenine, phosphatidylserine
805	807	Undetected	<i>Edge, Center</i>	-	Uracil
827	828	Undetected	<i>Edge, Center</i>	Protein	Phosphodiester in DNA
853	855	<i>Edge, Center</i>	<i>Edge, Center</i>	Glucose, potassium citrate	Tyrosine, proline, polysaccharides
876	882	Undetected	<i>Edge, Center</i>	Phosphate, human mucin I	Choline, phospholipids
924	923	Undetected	<i>Edge, Center</i>	Phosphate, glucose and protein (proline), lactic acid	-
957	959	<i>Edge</i>	<i>Center</i>	Protein	Hydroxyapatite
1003	1001	<i>Center</i> (broader and <i>Edge</i> narrower)	<i>Edge, Center</i>	Phenylalanine/protein, urea	NADH
1031	1032	<i>Center, Edge</i>	<i>Center, Edge</i>	Protein (phenylalanine)	Phospholipids
1045	1048	<i>Edge</i> (weak), <i>Center</i>	<i>Edge</i> (weak), <i>Center</i> (strong)	Nitrate and protein (phenylalanine), uric acid, lactic acid, human mucin I	Phosphate, carbohydrate
1082	1078	<i>Edge, Center</i> (weak)	<i>Center</i> (weak)	Protein, glucose	Carbohydrates, nucleic acids, phospholipids
1101	1098	<i>Edge</i>	<i>Edge, Center</i>	Protein	C-N, lipids
1125	1128	<i>Edge, Center</i> (weak)	<i>Edge, Center</i>	Protein	Lipid, RNA (ribose), carbohydrate, blood, porphyrin
1173	1172	<i>Edge, Center</i> (weak)	<i>Edge, Center</i>	Protein (tyrosine), urea	Carotenoids
1203	1208	<i>Center</i> (weak)	<i>Center</i> (weak)	-	Nucleic acids, amine III

1250	1254	Undetected	<i>Edge, Center</i>	Protein (amide III) , Human Mucin I	Asymmetric phosphate, DNA/RNA (guanine, cytosine), Nucleic acids, fatty acids
1319	1328	<i>Edge</i>	<i>Edge, Center</i>	Protein (amide III)	Nucleic acids (guanine)
1338	1338	<i>Edge, Center</i>	<i>Edge, Center</i>	Protein (amide III)	Nucleic acids
1338	1347	<i>Edge, Center</i>	<i>Edge, Center</i>	Protein (amide III)	Nucleic acids
1417	1417	<i>Center</i>	<i>Edge (weaker), Center (stronger)</i>	-	Aspartate, glutamate
1449	1448	<i>Edge (strong), Center</i>	<i>Edge, Center</i>	Protein (amide I),lactic acid	Lipid, red blood cells, aromatic carbonds
1512	1511	Undetected	<i>Edge, Center</i>	-	DNA, cytosine
1553	1553	<i>Center (strong relative to Edge), Edge (very weak)</i>	<i>Edge, Center</i>	Protein (tryptophan, amide II),sodium chloride	Mucin, porphyrin
1584	1578	<i>Edge</i>	<i>Edge,Center</i>	Citrate	Phenylalanine, carotenoids, DNA/RNA
1605	1605	<i>Edge</i>	<i>Edge, Center</i>	Protein (amide I)	DNA
1616	1611	<i>Edge</i>	<i>Edge, Center (in shoulder of peak)</i>	Protein (tyrosine, tryptophan)	Porphyrin
1665	1668	Undetected	<i>Edge, Center</i>	Protein (amide I),	Unsaturated fatty acids, DNA

30 The complementary cohort characteristics extracted from the questionnaire are tabulated in  
 31 Table 3.

32 **Table 3. Advanced clinical characteristics of the cohort. The characteristics are**  
 33 **separated by different categories such as: Disease, Nicotine Consumption,**  
 34 **Alcohol Consumption, Caffeine Consumption and Prescription**  
 35 **medication/vitamins. The characteristics were given by the volunteers, by**  
 36 **responding to a questionnaire.**

37		Yes [N] (n [%])	No [N] (n [%])	Statistic Not Given [N] (n [%])
38	<i><b>Disease</b></i>	-	-	-
39	Heart disease	3 (1.86)	156 (96.9)	2 (1.24)
40	Hypertension	10 (6.21)	149 (92.55)	2 (1.24)
41	Diabetes	4 (2.48)	155 (96.27)	2 (1.24)
42	Lung condition	14 (8.70)	145 (90.06)	2 (1.24)
43	Autoimmune	6 (3.73)	153 (95.03)	2 (1.24)
44	Neurological	4 (2.48)	154 (95.65)	3 (1.86)
45	Thyroid	14 (8.70)	144 (89.44)	3 (1.86)
46	Cancer	7 (4.35)	151 (93.79)	3 (1.86)
47	Oral disease	3 (1.86)	156 (96.89)	2 (1.24)
48	<i><b>Nicotine Consumption</b></i>	-	-	-
49				
50	None	148 (91.93)	13 (8.07)	-
51	Smoking	9 (5.59)	152 (94.41)	-
52	Vaping	4 (2.48)	157 (97.52)	-
53	Both	2 (1.24)	129 (98.76)	-
54	<i><b>Alcohol Consumption</b></i>	113 (70.19)	45 (27.95)	3 (1.86)
55	<i><b>Caffeine Consumption</b></i>	144 (89.44)	17 (10.56)	-
56	<i><b>Prescription medication or vitamins taken</b></i>	107 (66.46)	53 (30.92)	1 (0.62)